Syn- and post-eruptive erosion, gully formation, and morphological evolution of a tephra ring in tropical climate erupted in 1913 in West Ambrym, Vanuatu

Károly Németh[ab] and Shane J. Cronin[a]

[a]Massey University, Institute of Natural Resources, P.O. Box 11 222, Palmerston North, New Zealand, (k.nemeth@massey.ac.nz; s.j.cronin@massey.ac.nz)

[b]Geological Institute of Hungary, Department of Mapping, Stefánia út 14, H-1143, Budapest, Hungary

In press in Geomorphology

Please cite this article as:

Károly Németh, Shane J. Cronin, Syn- and post-eruptive erosion, gully formation, and morphological evolution of a

tephra ring in tropical climate erupted in 1913...,

Geomorphology (2006), doi:10.1016/j.geomorph.2006.08.016

Abstract

Syn- and post-eruptive erosion of volcanic cones plays an important role in mass redistribution of tephra over short periods. Descriptions of the early stages of erosion of tephra from monogenetic volcanic cones are rare, particularly those with a well-constrained timing of events. In spite of this lack of data, cone morphologies and erosion features are commonly used for long-term erosion rate calculations and relative age determinations in volcanic fields. This paper offers new observations which suggest differing constraints on the timing of erosion of a tephra ring may be operating than those conventionally cited. In 1913 a tephra ring was formed as part of an eruption in west Ambrym Island, Vanuatu and is now exposed along a continuous 2.5 km long coastal section. The ring surrounds an oval shaped depression filled by water. It is composed of a succession of a phreatomagmatic fall and base surge beds, interbedded with thin scoriaceous lapilli units. Toward the outer edges of the ring, base-surge beds are gradually replaced in the succession by fine-ash dominated debris-flows and hyperconcentrated-flow deposits. The inter-fingering of phreatomagmatic deposits with syn-volcanic reworked volcaniclastic sediments indicates that an ongoing remobilisation of freshly deposited tephra was already occurring during the eruption. Gullies cut into the un-weathered tephra are up to 4 m deep and commonly have c. 1 m of debris-flow deposit fill in their bases. There is no indication of weathering, vegetation fragments or soil development between the gully bases and the basal debris flow fills. Gully walls are steep and superficial fans of collapsed sediment are common. Most gullies are heavily vegetated although some active (ephemeral) channels occur. These observations suggest that the majority of the erosion of such tephra rings in tropical climates takes place directly during eruption and possibly for only a period of days to weeks afterward. After establishment of the gully network, tephra remobilisation is concentrated only within them. Therefore the shape of the erosion-modified volcanic landform is predominantly developed shortly after the eruption ceases. This observation indicates that gully erosion morphology may not necessarily relate to age of such a landform. Different intensities of erosion during eruption (related to water supply or rainfall) are probably the major influence on gully spacing, modal depth and form. Longer-term post-eruption processes that could be indicators of relative age may include internal gully deepening (below basal debris-flow fill sediments) and possibly widening and side-slope lowering due to undercutting and side-collapse.

Keywords: tephra ring, phreatomagmatic, maar, scoria, base surge, debris flow, mud flow, gully, Ambrym

1. Introduction

Tuff rings or cones are a common feature of basaltic volcanic fields. They are constructed via explosive magma-water interactions, known as phreatomagmatic eruptions (Zimanowski, 1998). Tuff cones/rings are typically comprised of well-bedded tephra layers of highly variable and contrasting sorting and particle-size characteristics (Rosi, 1992). These units are mostly deposited in a semi-saturated state and particularly the fine-ash dominated beds can form compact, cement-like, poorly permeable layers (Rosi, 1992). The entire cone is typically rapidly lithified through processes such as palagonitisation, hence their definition as "tuff". In some conditions, and when freshly erupted, such deposits are not lithified; in this case they are known as tephra cones/rings (ref). Even in a non-lithofied state, the contrasts in bed characteristics and the high component of poorly sorted and fine-ash rich layers in tephra rings gives them very different erosive properties compared to typically well-sorted and highly permeable scoria cones.

Volcaniclastic sedimentary successions within and around the margins of tuff rings are common and may result from either syn- or post-eruptive erosion (Sohn and Chough, 1989; Chough and Sohn, 1990). Immediate post-eruptive erosion is thought to be dominated by gully formation (Ollier and Brown, 1971), which apparently plays the most important role in mass redistribution of tephra from primary cones. Despite these features being widely recognised, the description of short-lived erosion processes from tephra cones with good constraints on the timing of events is relatively rare (Ollier and Brown, 1971). By contrast the erosion of scoria cones is better documented (Wood, 1980b; Wood, 1980a; Hooper and Sheridan, 1998), although even for these, the role of primary eruptive processes in the morphological development of scoria cones has only recently been addressed (Németh, 2004).

In spite of the lack of data on the syn-eruptive erosion or initial state of tephra cones or rings, their erosional morphologies are commonly used for relative-age dating in volcanic fields (e.g. Cronin and Neall, 2000) and also long-term erosion-rate calculations (Németh and Martin, 1999).

Phreatomagmatism, producing tuff/tephra rings and cones is an important eruption style of many historic eruptions on ocean islands (Cole et al., 1999) such as Ambrym in Vanuatu. At the western edge of Ambrym (Fig. 1), a phreatomagmatic volcanic field was formed in 1913 during a flank eruption (Gregory, 1917; McCall et al., 1969). This series of events produced seven tuff and scoria cones to cover an area of 25 km^2 (Gregory, 1917). One of these centres is particularly well exposed by coastal erosion and this together with eruption descriptions, enables inferences to be made of the syn- and immediate post-volcanic erosion processes of this tephra ring. Through sedimentological study of the tephra ring in relation to its vent geometry semi-quantitative constraints can be developed for the timing of the main phases of erosion of tuff rings/cones.

2. Tephra cone erosion forms and processes

Very little information is available on the erosion of tephra beds associated with phreatomagmatic volcanoes especially in tropical climates with high rainfall. Hence information from other environments must be considered. Wave-cut erosion has been well described around newly formed sub-lacustrine or shallow marine tuff cones including: Barcena, Mexico (Richards, 1959), Capelinhos, Portugal (Machado et al., 1962), or Lake Karymskoye, Kamchatka (Belousov and Belousova, 2001). These sub-aqueous structures can be very short lived, such as that of Graham Island/Ferdinadea which formed about 40 km from the southern coast of Sicily in 1831 (Calanchi et al., 1989; Caracausi et al., 2005; Rotolo et al., 2006). The island grew c. 50 metres above the sea level in 8 days, but it was eroded away 19 days later.

Tuff cones and scoria cones in arid and intracontinental settings show evidence for very little immediate tephra redistribution (Keller, 1973, White, 1991, Hooper and Sheridan, 1998). On flanks of cones in the San Francisco Volcanic Field, Arizona Hooper (1999) showed that scoria particles moved about 16 cm/a (Hooper, 1999). At the Parícutin scoria cone (Mexico) only 5.3% of deposits were redistributed in the 62 years from the onset of the eruption (Hooper, 2004). Some of this redistribution may be due to wind erosion, which is able to move fine basaltic tephra easily in arid climates (Arnalds et al., 2001).

Studies on newly exposed and tephra covered volcanic flanks following the 1980 eruption of Mount St Helens showed that infiltration was strongly reduced on the altered landscape (Major and Yamakoshi, 2005). Thick tephra mantles were shown to reduce infiltration initially as much as 50-fold. After 20 years the revegetated area has improved infiltration, but it remains the pre-eruptive levels. Due to this, high-magnitude, low-frequency storms and unusually rapid snowmelt still induces excessive overland flow.

3. Geological Setting and Morphology of the Tephra Cones

Ambrym is one of the most voluminous active volcanoes in the Vanuatu arc (Fig. 1). It is a triangular 35 x 50 km island, formed around an active E-W-oriented fissure zone, which is covered by many scoria cones and fissure fed lava flows (McCall et al., 1969; Carney et al., 1985). The northern part of the volcano is considered to be oldest and it is inferred to be part of an old shield volcano cross-cut with fissure vents (McCall et al., 1969). The central part comprises a 12 km-wide caldera, at between 600-800 m above seal level. Present day activity is concentrated at two active vent complexes Marum and Benbow (Fig. 1). These systems regularly produce small-volume Strombolian style events, phreatomagmatic explosions and more rarely sub-Plinian, and Vulcanian style eruptions (Wiart, 1995). Tephra from these frequently active centres along with periodic (including historic) intra-caldera lava flows have formed a large flat ash-plain in the caldera as well as several sediment-choked fluvial systems leading out from the caldera and down to the coast. The caldera formation is currently under debate, with a passive collapse mechanism (McCall et al., 1969) appearing more reasonable than a theory proposed later which involves a cataclysmic phreatomagmatic eruption (Robin et al., 1993). The first mechanism is supported by the typical nature of historic eruptions which have involved the passage of degassed basaltic magmas along lateral dykes down the E and W rift arms to feed flank eruptions (Wiart, 1995).

At the western and eastern extremities of Ambrym, many phreatomagmatic eruption centres developed near sea level as a result of interaction of fissure–fed magma and near surface water and/or water saturated sediments. The resulting tephra rings/cones typically have 1000 m diameter craters and low (<100 m) rims. The most recent eruptions took place in 1894 and 1913 at the western edge of Ambrym (Purey-Cust, 1896; Frater, 1917; Gregory, 1917).

One of the 1913 rings is cut by a coastal cliff, exposing a 15 m-thick phreatomagmatic tephra sequence. This tephra ring surrounds an oval-shaped depression (1200x600 m) containing a shallow lake (Fig. 2). There is a partial opening in the NW side, where sea water inundation occurs during cyclone storm surges. The ring crest reaches 85 m in the north (Fig. 3) and its outer flanks have gentle slopes (5-10°) over a lateral distance of c. 600 m. At its eastern side the tephra layers of the ring mantle older lava flows scoria cones (Fig. 3). On its western side, the ring grades into a low volcaniclastic debris fan. This ring is similar in broad geometry to other young tephra/tuff rings worldwide, having wide craters with relatively low crater rims. Tephra deposits extend approximately 1 km outward of the crater rim. There are no characteristic erosion scars or gullies visible on the upper outer flanks of the ring; they become prominent only by c. 700 m away from its rim.The feature was reported as new land (Frater, 1917), indicating that the eruption was initially seated in shallow subaqueous conditions, probably on a coral reef. Hence coral fragments are common throughout the deposits, with some horizons being particularly rich. The entire structure is uniformly covered by dense forest of casurina with trunk diameters up to 40 cm, along with various shrub species.

4. Climate of study site

Vanuatu has a tropical maritime climate with uniform temperatures and high humidity (>80% average). A dry season occurs between May to October, with a wet (and warmer) season between November and April. The warmest month is February and the coolest is August. In the coastal locations, daily temperatures average 26 °C (wet season) and 24 °C (dry) with extremes between 33 °C and a night-time minimum of 13 °C (Anon, 1994).

Rainfall averages c. 2300 mm/a over the archipelago, but is highly variable depending on location and season. In the wet season, the Inter Tropical Convergence Zone is one of the main rainfall producing systems, particularly for the northern islands. In La Nina years, the South Pacific Convergence Zone also generates greater rainfall. For larger islands, such as Ambrym, orographic effects generate higher rainfall in the SE parts, with significantly drier conditions (particularly during dry season) in the W and NW regions – such as the study site.

By comparison, on the island of Efate (to the south), rainfall varies between 2400-3000 mm/a on the windward side, with 1000-1500 mm/a on the dry side and >4000 mm/a in elevated areas (Anon, 1994).

The SE trade winds are typically constant at 10 knots during the dry season (ranging up to 25 knots), however, the study site is sheltered from these. Winds of the wet season are light and variable, but cyclones are common. Vanuatu is affected by about 20 to 30 cyclones per decade, with 3 to 5 causing severe vegetation and landscape damage through strong winds and heavy rainfalls. Ambrym has been strongly affected on at least 6 occasions since 1847 but has also experienced the fringe effects of many of the other events (VMS, 1994). Cyclone Ivy in 2004 was the latest to directly affect Ambrym and it caused widespread flooding and landslides, along with strong coastal erosion at the study site.

5. Tephra ring succession

Near the western tip of Ambrym, a near continuous coastal cliff section exposes an up to 15 m thick succession of volcaniclastic units, dominantly phreatomagmatic tephras. This section cuts through a tuff ring around the northernmost of the 1913 vents (Fig. 3). The succession can be subdivided into 4 major lithostratigraphic units (Fig. 4):

1. PH1 forms a basal succession of lapilli and ash beds composed of weakly to moderately bedded, poorly sorted, cross-bedded to dune bedded tephra up to 10 m in thickness (Fig. 5a). These deposits contain abundant coral fragments, indicating that the fragmentation level of magma-water interaction must have been in a coral reef or coral-rich gravel near the pre-eruption shoreline. Proximal base-surge beds are volumetrically dominant in this unit (Fig. 5b), interbedded with explosion-breccia horizons associated with more

vigorous vent-clearing phases of the eruption (c.f., Houghton and Schmincke, 1989; Houghton et al., 1996). Overall, PH1 has a lensoid geometry in three dimensions, forming the foundations of a prominent tephra ring.

2. Overlying PH1 is a metre-thick, clast-supported, scoria fall deposit MF (Fig. 5c). Its clasts are flat, angular, and highly vesicular, with irregular shape vesicles, all suggesting a magmatic degassing-driven fragmentation of the uprising melt (c.f., Houghton et al., 1996; Houghton et al., 1999). The unit can be subdivided into at least five (0.1-0.5 m thick) sets of coarse-medium lapilli, each overlain by few cm-thick, laminated fine ash. The beds are non-graded, moderately sorted with weak stratification. The unit mantles PH1 with a fairly uniform thickness, suggesting its air fall origin (c.f., Wilson and Houghton, 2000).
3. PH2 (Fig. 5d) is a 10 m sequence of tephra that overlies MF. It can be subdivided into 3 major sub-units, each containing a coarse accidental lithic breccia-bearing ash to lapilli horizon (Fig. 5d). The accidental lithic fragments are predominantly coherent lava rocks from pre-eruptive mafic lava units as well as indurated phreatomagmatic lapilli tuff fragments. Some of the blocks up to 1.5 m in diameter with impact sags of 20-40 cm are ballistic bombs. These 0.5-1.5 m thick accidental-lithic-rich beds are overlain by a metre-thick succession of cross-bedded to dune-bedded ash and lapilli beds, interpreted to be high-to-low particle concentration base surge deposited units (after Waters and Fisher, 1971; Chough and Sohn, 1990; Bull and Cas, 2000) (Fig. 5d). Accretionary lapilli are common in the finer-grained units of this succession.
4. The TR unit is similar, but greater in thickness to MF (Fig. 6). The contact between PH2 and TR is gradational with a broad (about 1 m-wide) transition zone, indicating that the formation of these two units closely linked (Fig. 6). Abundant coral fragments and scoria lapilli are the main constituents of this unit, which has the mantling and sorting

characteristics of a fall unit (Fig. 6). TR is interpreted to be a localized scoriaceous tephra ring that was covered by the tephra deposits of PH2.

The tephra ring succession is interpreted to be deposited predominantly from pyroclastic density currents (surges and pycroclastic flows) and deposited as the currents gradually lost energy, as well when tephra fell into the passing base surge currents (Dellino et al., 2004a). The interbedded 1 m thick scoriaceous fall (MF) is interpreted to be a result from an intermittent change in eruptive style, where water availability to fuel magma-water interaction was suppressed (Houghton et al., 1999). The tephra ring is in semi-consolidated state today, with a stable upper surface. Wave-induced erosion causes frequent collapse of shoreline cliffs, especially during storm surges associated with cyclone events. These cliffs form excellent vertical exposures through the tuff ring at a sub-perpendicular orientation to radial gullies on the tephra ring.

6. Syn-eruptive reworked deposits

In laterally distal sections (several 300-500 m away from the rim) the primary base-surge dominated succession of PH2 is progressively replaced by a succession of 0.2-0.5 m thick beds of reworked tephra (Fig. 7). These deposits intercalate with the primary units and were obviously deposited during syn-volcanic reworking of fine ash from the tuff ring sides. This reworked tephra quickly formed debris flows and/or hyperconcentrated mass flows (Chough and Sohn, 1990; Lajoie et al., 1992).

The reworked units comprise 0.2-to-1 m scale beds, lying sub-horizontal, commonly with sharp and flat-lying contacts (Fig. 7). There are no impact sags or accretionary lapilli in this part of the succession. The beds are laterally continuous over tens of metres and bed thickness is commonly uniform over 20-30 m of lateral exposure. At sites 200-300 m from the rim crest (Fig. 7) massive, boulder-rich debris flow deposits occur and can be c. 1 m thick. Moving farther away, beds are on the order of 0.2-0.4 m in thickness, and are massive to weakly stratified, matrix supported, gravely sands (Fig. 8A). Tabular cross-bedding is occasionally visible, indicating that some of the flows became in some cases more dilute with distance to form watery run-out flows from the original hyperconcentrated mass-flows (c.f. Cronin et al., 2000).

In the most distal exposures (Fig. 8A), c 500 m from the tephra ring crest, massive matrix-supported fine gravely sands dominate the section, deposits characteristic of sandy hyperconcentrated flows (Cronin et al., 1999). Intercalated few cm-thick, poorly sorted, undulating, matrix supported ash deposits represent the distal ends of primary phreatomagmatic base-surge deposits (Fig. 8A). Mud drapes of a few mm-cm cover each of the tabular hyperconcentrated flow beds, indicating that the depositional system was water-saturated and post-emplacement settling and elutriation of fines occurred between successive flows (Fig. 8B). Mud drapes formed by such settling processes were observed to take 1-2 hours to form as hyperconcentrated deposits of similar particle size distribution settled post-emplacement (e.g. Cronin et al., 2000).

The inter-fingering of phreatomagmatic deposits with syn-volcanic reworked volcaniclastic sediments indicates an ongoing remobilisation of freshly deposited tephra, especially during the latter stages of the eruption.

7. Tephra-ring erosion and gully formation

The northern shoreline of the 1913 tephra ring in Ambrym follows the semicircular architecture of the tephra ring. Until recently, the succession was covered by heavy vegetation, but two recent tropical cyclones caused strong coastal erosion, creating continuous vertical cliff exposures. This section effectively provides a 2 km-long lateral cross section sub-normal to the flow direction of base-surges and pyroclastic density currents. The exposures show gully forms and tuff ring sequences between c. 500 m and 1500 m from the inferred elongated vent system within the Lake Fantang area (Fig. 1). They range between <100 and 800 m outside the rim of the tuff ring.

Early and mid eruption erosion processes

Whilst the distal deposits described above clearly show evidence of significant syn-eruptive deposition, the primary deposits of the tuff cone sequence, especially PH1, MF and the lower parts of PH2 show very little obvious evidence for erosion within or between units. Beds are continuous over lateral exposures of >400 m, with contacts being often sharp and even. Minor undulations and erosion, mostly forming irregularities on the scale of <0.3 m is evident where base-surges or pyroclastic density current scoured still-saturated substrates during passage. Deposits of these units often also contain rip-up clasts of underlying beds. However the processes feeding sediment into mostly fine-grained debris and hyperconcentrated flows into the distal areas appears to be:

1. Condensation of primary surges/pyroclastic density currents into wet lahars (c.f. Cronin et al., 1997);

2. and/or, sheet erosion of lower tuff-cone slopes between deposition events by syn-eruptive rainfall or liquefaction and remobilisation of saturated primary deposits.

The mud flows and debris flows in the distal areas form tabular beds 0.2-0.5 m in thickness, mantled by predominantly base-surge generated tephra deposits. These syn-eruptive processes were very important in sediment redistribution from the tuff ring as well as significantly changing the surrounding landscape (by creating a broader apron in places around the tephra ring). However, it is important to note that during most of the cone/ring-forming eruptions that large-scale gullying and erosional-scar formation within the tephra ring was not occurring.

Late and post-eruption erosion processes

The most significant difference in the depositional record of the lower tuff ring and that of the upper part is the presence of major gullies cut into the tephra sequence of TR and PH2.

In the 2 km long section, at least 26 >1 m deep gullies occur, including 11 >3 m in depth. The deepest is 6 m, and is cut into almost the entire primary tephra succession. The gullies are typically immature forms with 80% of them having width/depth rations between 2 to 3. The gullies are cut into predominantly flat-lying beds and typically without primary tephra deposits draping their sides. In two examples, minor primary draping and infilling deposits (e.g. Fig. 9B and 10A) occur on gully sides implying ongoing eruption at least during initiation of gully erosion. There is no soil horizon or evidence of weathering on the top of the tephra units at the gully bases, suggesting no significant time break between gully formation and partial infilling. This, together with the lack of primary deposit drapes in most gullies implies either that gully deepening was significant post eruption and thus removed any draping primary deposits, or that at least some of the gullies were started post-eruption.

There are two types of gully cross-sectional forms found in proximal exposures (100-300 m laterally outside the tephra ring-crest); 1) broad and relatively shallow U-shaped gullies (Fig. 9A); and a 2) steep, narrow gullies also with a basal U-shape (Fig. 9B). The broadest gully exposed is 15 m wide, in contrast to the more-common narrow gullies that are on the order of 2-5 m wide. In the distal exposures of the tephra ring, >500 m from the ring-crest, gullies are of only one type. They are shallower, commonly forming only a small and smooth depression over the tephra succession (Fig. 9C).

Distal exposure gullies are typically fully covered by a vegetation mat of at least 20 cm in thickness (Fig. 9C). Proximal gullies are also mostly heavily vegetated and stable in form (Fig. 9D). In most gullies, up to 1 m thick debris-flow and hyperconcentrated mass-flow deposits fill the basal parts of the gully (Fig. 10A). Some of the debris flow deposits contain clasts up to 1 m size; these are volcanic bombs, and blocks of semi-consolidated tephra beds from the tephra ring (Fig. 10A). In steep gullies, wall-collapses are common (Fig. 10B). These appear to have formed soon after gully deepening, since the collapsed walls are commonly preserved by vegetation growth of the same age and form as un-collapsed walls. The fill sediments, collapsed debris from walls and intact gully sides are all overlain by a thin humic soil layer and vegetation mat. Similarly interfluves and flanks of the tephra ring are vegetated in the same fashion, including trees with trunk diameters of up to 50 cm. The tephra ring is completely and evenly vegetated from its rim to the distal lower flanks. Many of the gully floors probably act as ephemeral channels during heavy rainfall events, despite being fully vegetated.

The vegetation and erosion pattern suggests that the tephra remobilisation and gully formation must have been intense for a short period, but has now effectively stopped. From the sedimentological evidence of intercalating hyperconcentrated flow deposits and primary eruptives at the edges of the ring, it appears that the erosion was intense near the end of the eruption and immediately following it. The lack of significant younger reworking and even remobilisation of the hyperconcentrated deposits shows that the rapid colonisation of the land by vegetation very quickly led to stabilisation of the tephra ring. Hence, even under the humid tropical climate conditions, and with frequent cyclones, the gully forms are essentially the same as their immediate post-eruption state.

Major and Yamakoshi's (2005) study at Mt St Helens highlighted the fact that thick tephra cover could initiate intense surface runoff and intensify gully erosion over the bare tephra covered landscape. This process is likely to be particularly important at Ambrym where rainfall intensities are high and cyclone events common. Rain storms during the latter stages of the eruption, or soon afterward could have generated the conditions for overland flow and initial carving of the gullies. These storms may have even been eruption-related since several observed ash-eruptions have induced instability in the immediate atmosphere, often precipitating local electrical storms and heavy rain falls (Blong, 1984).

From a comparable environment, the Ilchulbong tuff cone of Cheju Island, Korea shows two major lithofacies associations identified with mass wasting (Sohn and Chough, 1992). Lenticular and hummocky beds of massive stacked deposits intercalated between crudely to thinly stratified lapilli tuffs mark the base of slope. These beds were interpreted to represent occasional resedimentation of tephra by debris flows and slides during the eruption (Sohn and

Chough, 1992), in a similar fashion to the coarse breccia interbeds identified in the succession described here at Ambrym. In distal areas at Ilchulbong, massive, inversely graded and cross-bedded gravelly sandstones are inferred to represent post-eruptive reworking of tephra by debris and stream flows (Sohn and Chough, 1992). These beds have a very similar architecture to the distal reworked volcaniclastic units described at the Ambrym tuff ring. However, here the different facies are interpreted to represent proximal-distal transitions in flow character of coeval flows (dilution in sediment content with distance) rather than different periods of deposition.

Few quantitative data delimit the immediate erosional forces acting immediately after the formation of tuff cones and rings. At Barcena tephra cone in Mexico, 10 m deep, dry valleys formed just few months alter the eruption under around half the average annual rainfall as Ambrym (Richards, 1965; White, 1991). The Rininahue maar in Chile underwent significant fluvial erosion weeks after its eruption (Müller and Veyl, 1956), although since then the remains of the ring are stable, dissected by gullies and covered by scrub vegetation. It appears that harder inter-beds in the phreatomagmatic tephra successions (Rosi, 1992), immediately form hard surface crusts over large surface areas which can stabilise the volcanic landform relatively quickly and allow time for deeper drainage and tephra compaction and alteration. Acting against this, however, would be the event of torrential rain falls while the tephra beds are still in a semi-saturated state, i.e., immediately after deposition. A recent example of this, under an extremely high-rainfall climate, is a small tuff cone developed within a crater lake at c. 1200 m elevation on Ambae volcano (Vanuatu). This developed during early-mid December 2005 in the middle of the wet-season, and several rainstorms accompanied and followed the main period of activity (Németh et al., 2006). Aside from the wave-cut erosion, small gully systems had developed on the outer flanks of this cone within days of the cessation of eruption along with coalescing fans of eroded tephra built up around the cone (Fig. 11). The sizes and spacing of gullies are significantly smaller than the west Ambrym cone studied here, but then the Ambae cone is significantly smaller and its slope angle higher (~ 20° versus < 5-10°).

8. Erosion styles and implications for geomorphic dating

This 1913 tephra ring architecture shows sheet-style deposition dominating in distal areas, where tabular beds of primary (from surge and pyroclastic density current) and secondary deposits (from sandy hyperconcentrated mass flow and debris flow) are interbedded. This distal sequence was clearly formed by syn-eruptive reworking of sediment from higher parts of the growing tuff ring. By contrast, in the proximal sites, no deposition of reworked material occurs and little evidence for any erosion is evident in the primary surge and pyroclastic density current deposits recording the main development of the tuff ring. Only in the latest-formed deposits of the ring are large-scale gullies evident. These are cut into the upper parts of the primary deposit sequence, and were hence formed in the very latest stages of the eruption and probably significantly deepened during a short period of intense gully erosion immediately following eruption.

Once formed, this network of gullies clearly played an important role in channelling rainwater down the flanks of the volcano. However, even under the conditions of this humid tropical climate, once vegetated, the gullies have remained very stable in form. In the example we document, there is no evidence for significant sheet or gully erosion on the flanks of the tuff ring soon after vegetation cover was established. Tiny, cm-scale rock pillars under a vegetation mat indicate that small-scale sheet erosion occurs, possibly during exceptionally heavy rainfall or cyclone events. These surficial processes appear, however, not to have played a significant role in the modification of the tephra ring's original shape.

The gully network on this tuff ring is not as well developed as those described in other steeper volcanic cones, such as Vulcan in Papua New Guinea (Ollier and Brown, 1971). This appears due to the different textural characteristics of the deposits of Vulcan and the 1913 Ambrym tephra ring. Vulcan is a scoria cone, reportedly with very homogeneous and highly permeable scoria lapilli beds that form an almost perfectly shaped cone with slopes at the repose angle of the lapilli (Ollier and Brown, 1971). This cone was quickly eroded, and a complex gully network developed in the first decade of the volcano's existence (Ollier and Brown, 1971). At Ambrym, the tephra ring is significantly lower, and mostly with only gentle slopes (< 10). In addition, the tephra beds that make it up have very different sorting, particle size distribution, compaction and permeability characteristics to bedded scoria. The alternation of highly variable bed types can lead to features such as thin, compact fine-grained layers armouring more readily-reworked units below. It may also lead to perching of water in sub-surface horizons and even development of high hydrostatic pressures to generated deeper failures in the cone deposits. Hence, the strong variability in grain size and textural characteristics of the beds making up the ring also favoured the development of an irregular erosional pattern.

The main deposit types in tuff rings include very poorly sorted coarse-block bearing tuff horizons, firmly compacted fine ash beds and friable scoria lapilli beds. Some of the finer-grained, accretionary lapilli bearing tuffs form particularly hard beds up to 25 cm thick. These very likely play an important role in controlling pore water movement through the volcanic edifice as well as being strongly resistant to surface runoff. This effect is particularly strong following rapid diagenetic processes which harden the beds still further, stabilising the tuff-ring flanks. The poor sorting characteristics of the phreatomagmatic tuffs also hinder effective infiltration and subsurface water flow, which also strongly controls how erosion may start on the flanks. The importance of such textural variations in the erosion processes acting on pyroclastic successions of phreatomagmatic volcanoes was also pointed out during studies of the long term erosional pattern of tuff rings in subaerial settings (White, 1991). With much older units studied by White (1991) it was concluded that the initial condition of the tephra ring as well as the climate plays the most important role how erosion will continue in such volcanoes. Our results indicate that it is the most important processes controlling phreatomagmatic volcano shape are erosion forms that occur during the very last stages of eruption and immediately following it. Once vegetation is established, very little long term change appears to occur. This is not only true for the 1913 cones, but nearby vents from an 1876 and other late Holocene eruptions on Ambae show similar cone morphologies to the 1913 events. These implications are important for studies where the morphology of cones is used to establish patterns of relative age relationships in monogenetic volcanic fields (e.g. Hasenaka and Carmichael, 1985; Cronin and Neall, 2001). Our findings suggest that it is the immediate post-eruption erosion that is important and longer term processes are likely to only exert a very minor influence on the morphology of phreatomagmatic cones and tuff rings.

9. Conclusion

On the basis of field observations of a tephra ring formed 1913 in West Ambrym, Vanuatu, we have elucidated the timing and nature of erosion processes that give rise to the typical morphological characteristics of phreatomagmatic cones and rings. The low slope angles of the flank and the diameter of the ring in relationship with the crater diameter are very similar to other tephra rings described in many different settings (Heiken, 1971; Fisher and

Schmincke, 1984; Cas and Wright, 1988; Vespermann and Schmincke, 2000). Hence the processes we describe here are like to be broadly applicable to many areas of phreatomagmatic volcanism. We conclude that while sheet erosion may be important throughout the formation of such cones, gully erosion is only important in the very late stages of eruptions and immediately following them. The variations in texture of tephra succession in phreatomagmatic volcanoes include layers of poorly sorted or relatively firm fine-ash beds which are resistant to surface erosion. Following rapid vegetation of such cones in tropical areas, they become very stable, with even heavy rainfall events and cyclones not causing deepening of gullies or significant changes in the tuff cone shape, at least over the scale of 100's and perhaps a few thousand years. These observations together indicate that long-term erosion patterns of tephra rings should be interpreted in relation to age with care.

10. Acknowledgements

This work has been partly supported by FRST-PGST funding -MAUXO401 (SJC) and a NZ FRST Post-doctoral research grant - MAUX0405 (KN). Douglas Charley provided excellent logistical help during this work along with the custom landowners of this area. We are grateful for constructive reviews by two journal reviewers that helped to clarify many aspects of this paper.

11. References

Anon. (1994). Vanuatu National Agricultural Census. Statistics Office, Port Vila Vanuatu. 190 pp.

Arnalds, O., Gisladottir, F.O. and Sigurjonsson, H., 2001. Sandy deserts of Iceland: an overview. Journal of Arid Environments, 47(3): 359-371.

Belousov, A. and Belousova, M., 2001. Eruptive process, effects and deposits of the 1996 and the ancient basaltic phreatomagmatic eruptions in Karymskoye lake, Kamchatka, Russia. In: J.D.L. White and N.R. Riggs (Editors), Volcaniclastic sedimentation in lacustrine settings. Balckwell Sciences, Oxford, UK, pp. 35-60.

Blong, R.J., 1984. Volcanic hazards - A sourcebook on the effects of eruptions: Academic Press, Australia, 424 p.

Bull, S.W. and Cas, R.A.F., 2000. Distinguishing base-surge deposits and volcaniclastic fluviatile sediments: an ancient example from the Lower Devonian Snowy River Volcanics, south-eastern Australia. Sedimentology, 47(1): 87-98.
Calanchi, N., Colantoni, P., Rossi, P.L., Saitta, M. and Serri, G., 1989. The Strait Of Sicily Continental Rift Systems - Physiography And Petrochemistry Of The Submarine Volcanic Centers. Marine Geology, 87(1): 55-83.
Caracausi, A., Favara, R., Italiano, F., Nuccio, P.M., Paonita, A. and Rizzo, A., 2005. Active geodynamics of the central Mediterranean Sea: Tensional tectonic evidences in western Sicily from mantle-derived helium. Geophysical Research Letters, 32(4).
Carney, J.N., Macfarlane, A. and Mallick, D.I.J., 1985. The Vanuatu Island-Arc - An Outline Of The Stratigraphy, Structure, And Petrology. Ocean Basins And Margins, 7: 683-718.
Cas, R.A.F. and Wright, J.V., 1988. Volcanic succesions, modern and ancient. Chapman & Hall, London, 528 pp.
Chough, S.K. and Sohn, Y.K., 1990. Depositional mechanics and sequences of base surges, Songaksan tuff ring, Cheju Island, Korea. Sedimentology, 37: 1115-1135.
Cole, P.D., Guest, J.E., Queiroz, G., Wallenstein, N., Pacheco, J.M., Gaspar, J.L., Ferreira, T. and Duncan, A.M., 1999. Styles of volcanism and volcanic hazards on Furnas volcano, Sao Miguel, Azores. Journal of Volcanology and Geothermal Research, 92(1-2): 39-53.
Cronin, S.J., Neall, V.E., 2001: Holocene volcanic geology, volcanic hazard and risk on Taveuni, Fiji. New Zealand Journal of Geology and Geophysics 44: 417-437.
Cronin, S.J., Lecointre, J.A., Palmer, A.S. and Neall, V.E., 2000. Transformation, internal stratification, and depositional processes within a channelised, multi-peaked lahar flow. New Zealand Journal of Geology and Geophysics, 43: 117-128.
Dellino, P., Isaia, R., La Volpe, L. and Orsi, G., 2004a. Interaction between particles transported by fallout and surge in the deposits of the Agnano-Monte Spina eruption (Campi Flegrei, Southern Italy). Journal of Volcanology and Geothermal Research, 133(1-4): 193-210.
Dellino, P., Isaia, R. and Veneruso, M., 2004b. Turbulent boundary layer shear flows as an approximation of base surges at Campi Flegrei (Southern Italy). Journal of Volcanology and Geothermal Research, 133(1-4): 211-228.
Fisher, R.V. and Schmincke, H.-U., 1984. Pyroclastic Rocks. Springer, Heidelberg, 474 pp.
Frater, M., 1917. Volcanic eruption, Ambrym Island (1913). Geological Magazine, 6(4): 496-503.
Gregory, J.W., 1917. The Ambrym eruptions of 1913-1914. Geological Magazine, December 1917: 496-503.
Hasenaka, T., Carmichael, I.S.E. 1985: The cinder cones of Michoacàn-Guanajuato, central Mexico: their age, volume and distribution, and magma discharge rate. Journal of Volcanology and Geothermal Research 25: 105-124.
Heiken, G.H., 1971. Tuff rings: examples from the Fort Rock-Christmas Lake Valley Basin, South-Central Oregon. Journal of Geophysical Research, 76(23): 5615-5626.
Hooper, D.M., 1999. Cinder movement experiments on scoria cones slopes; rates and direction of transport. Landform Analysis (University of Silesia Press; Association of Polish Geomprphologists, Katowice, Poland), 2: 5-18.
Hooper, D.M., 2004. Geomorphological modeling of the long-term redistribution of tephra deposits. Geological Society of America Abstracts with Programs, 36(5): 283.
Hooper, D.M. and Sheridan, M.F., 1998. Computer-simulation models of scoria cone degradation. Journal of Volcanology and Geothermal Research, 83: 241-267.

Houghton, B.F. and Schmincke, H.U., 1989. Rothenberg scoria cone, East Eifel; a complex strombolian and phreatomagmatic volcano. Bulletin of Volcanology, 52(1): 28-48.
Houghton, B.F., Wilson, C.J.N., Rosenberg, M.D., Smith, I.E.M. and Parker, R.J., 1996. Mixed deposits of complex magmatic and phreatomagmatic volcanism: An example from Crater Hill, Auckland, New Zealand. Bulletin of Volcanology, 58(1): 59-66.
Houghton, B.F., Wilson, C.J.N. and Smith, I.E.M., 1999. Shallow-seated controls on styles of explosive basaltic volcanism: a case study from New Zealand. Journal of Volcanology and Geothermal Research, 91(1): 97-120.
Keller, J., 1973. Quaternary Maar Volcanism near Karapinar in Central Anatolia, Symposium on Volcanism and Associated Metallogenesis, Bucharest, pp. 378-396.
Lajoie, J., Lanzafame, G., Rossi, P.L. and Tranne, C.A., 1992. Lateral facies variations in hydromagmatic pyroclastic deposits at Linosa, Italy. Journal of Volcanology and Geothermal Research, 54: 135-143.
Machado, F., Parsons, W.H., Richards, A.F. and Mulford, J.W., 1962. Capelinhos eruptions of Fayal Volcano, Azores, 1957-1958. Journal of Geophysical Research, 67: 3519-3529.
Major, J.J. and Yamakoshi, T., 2005. Decadal-scale change of infiltration characteristics of a tephra-mantled hillslope at Mount St Helens, Washington. Hydrological Processes, 19(18): 3621-3630.
McCall, G.J.H., LeMaitre, R.W., Malahoff, A., Robinson, G.P. and Stephenson, P.J., 1969. The geology and geophysics of the Ambrym Caldera. New Hebrides, Symposium Volcanoes and Their Roots, Oxford, England, pp. 682-696.
Müller, G. and Veyl, G., 1956. The birth of Nilahue, a new maar type volcano at Rininahue, Chile. Congreso Geologico Internacional, Seccio I - Vulcanologia del Cenozoico: 375-396.
Németh, K., 2004. The morphology and origin of wide craters at Al Haruj al Abyad, Libya: maars and phreatomagmatism in a large intracontinental flood lava field? Zeitschrift für Geomorphologie, 48(4): 417-439.
Németh, K., Cronin, J.S., Charley, D., Harrison, M. and Garae, E., 2006. Exploding lakes in Vanuatu - "Surtseyan-style" eruptions witnessed on Ambae Island. Episodes [in press]
Németh, K. and Martin, U., 1999. Late Miocene paleo-geomorphology of the Bakony-Balaton Highland Volcanic Field (Hungary) using physical volcanology data. Zeitschrift für Geomorphologie, 43(4): 417-438.
Ollier, C.D. and Brown, M.J.F., 1971. Erosion of a young volcano in New Guinea. Zeitschrift für Geomorphologie, 15(1): 12-28.
Purey-Cust, H.E., 1896. The eruption of Ambrym Volcano, New Hebrides, South-West Pacific, 1894. Geographical Journal, VIII: 585-602.
Richards, A.F., 1959. Geology of the Islas Revillagigedo, Mexico, 1. Birth and development of Volcan Barcena, Isla San Benedicto. Bulletin of Volcanology, 22: 73-123.
Richards, A.F., 1965. Geology of the Islas Revillagigedo, 3. Effects of erosion on Isla San Benedicto 1952-1961 following the birth of Volcan Barcena. Bulletin Volcanologique, 28: 381-403.
Robin, C., Eissen, J.P. and Monzier, M., 1993. Giant Tuff Cone And 12-Km-Wide Associated Caldera At Ambrym Volcano (Vanuatu, New-Hebrides-Arc). Journal of Volcanology And Geothermal Research, 55(3-4): 225-238.
Rosi, M., 1992. A model for the formation of vesiculated tuff by the coalescence of accretionary lapilli. Bulletin of Volcanology, 54: 429-434.
Rotolo, S.G., Castorina, F., Cellura, D. and Pompilio, M., 2006. Petrology and geochemistry of submarine volcanism in the Sicily Channel Rift. Journal of Geology, 114(3): 355-365.

Sohn, Y.K. and Chough, S.K., 1989. Depositional Processes of the Suwolbong Tuff Ring, Cheju Island (Korea). Sedimentology, 36(5): 837-855.
Sohn, Y.K. and Chough, S.K., 1992. The Ilchulbong Tuff Cone, Cheju Island, South-Korea - Depositional Processes And Evolution Of An Emergent, Surtseyan-Type Tuff Cone. Sedimentology, 39(4): 523-544.
Vespermann, D. and Schmincke, H.-U., 2000. Scoria cones and tuff rings. In: H. Sigurdsson, B.F. Houghton, S.R. McNutt, H. Rymer and J. Stix (Editors), Encyclopedia of Volcanoes. Academic Press, San Diego, pp. 683-694.
Waters, A.C. and Fisher, R.V., 1971. Base surges and its deposits: Capelinhos and Taal volcanoes. Journal of Geophysical Research, 76: 5596-5614.
White, J.D.L., 1991. The depositional record of small, monogenetic volcanoes within terrestrical basins. In: R.V. Fisher and G.A. Smith (Editors), Sedimentation in Volcanic Settings. Society for Sedimentary Geology, Tulsa (Oklahoma), pp. 155-171.
Wiart, P., 1995: Impact et gestion des risques volcaniques au Vanuatu. Notes Techniques, Sciences de la Terre, Geologie-geophysique, 13. ORSTOM, Vanuatu, 80 pp.
Wilson, C.J.N. and Houghton, B., 2000. Pyroclastic transport and deposition. In: H. Sigurdsson (Editor), Encyclopedia of Volcanoes. Academic Press, San Diego, pp. 545-554.
Wood, C.A., 1980a. Morphometric analysis of cinder-cone degradation. Journal of Volcanology and Geothermal Research, 8(2-4): 137-160.
Wood, C.A., 1980b. Morphometric evolution of cinder cones. Journal of Volcanology and Geothermal Research, 7: 387-413.
Zimanowski, B., 1998. Phreatomagmatic explosions. In: A. Freundt and M. Rosi (Editors), From magma to tephra. Elsevier, Amsterdam, pp. 25-53.

Fig. 1
A - Overview of the SW-Pacific.
B - Overview of Vanuatu volcanic arc.
C – D - Overview of Ambrym island
E - Enlargement of the 1913 eruption site. Thick grey line on coast represents the study site. Black thick line marks the tephra ring crater rim.

Fig. 2
Overview of the Lake Fantang maar lake from the east.

Fig. 3
Overview of the Lake Fantang maar from air from the north. Coastal section exposes about 2.5 km long distal succession of the phreatomagmatic tephra ring.

Fig. 4
Overview of the pyroclastic succession with PH1, MF1, PH2 close to the small low bank of the northern side of the Lake Fantang maar. Arrows point to gullies in cross section.

Fig. 5
A – base surge beds (bs) overlain by breccia horizon (bh) rich in accidental volcanic lithic bombs and blocks in PH1 unit. Hammer is in the circle.
B – pyroclastic breccia horizons in PH1 unit. Arrow points to the impact direction of a ballisticly emplaced volcanic lithic block.
C – scoriaceous tephra (MF) separates PH1 and PH2. Arrows point to coral fragments in the tephra beds (c). Hammer is in the circle.
D – overview of PH2 succession dominated by dune bedded base surge (db bs) beds. Arrow points to the impact direction of the volcanic lithic clast in the centre of the picture. Hammer is in the circle.

Fig. 6
Overview of the pyroclastic succession of TR. Dashed line shows the broad transition zone between PH2 and TR. Arrows point to small gullies cut into TR unit.

Fig. 7
Overview of reworked distal tephra section

Fig. 8
A – homogeneous, massive, grey volcaniclastic deposit in the distal section
B – alternating coarse grained sandy deposit with mud drapes (md – and arrows) indicative for water-rich depositional environment.

Fig. 9
A – broad, shallow gully
B – deep, steep gully
C – vegetation mat over shallow gully in distal section
D – heavy vegetation cover in gully floor

Fig. 10
A – debris flow deposit filling the gully floor
B – collapse textures in gully wall

Fig. 11
A – newly formed (December 2005) tephra cone in the Lake Vui caldera lake (Ambae Island, Vanuatu). Note the initial wave cut erosion marks on the shoreline of the new island.
B – aerial view of the newly formed (December 2005) Surtseyan tephra cone in Lake Vui (Ambae Island, Vanuatu) with straight immature gully network on its flank (arrows).

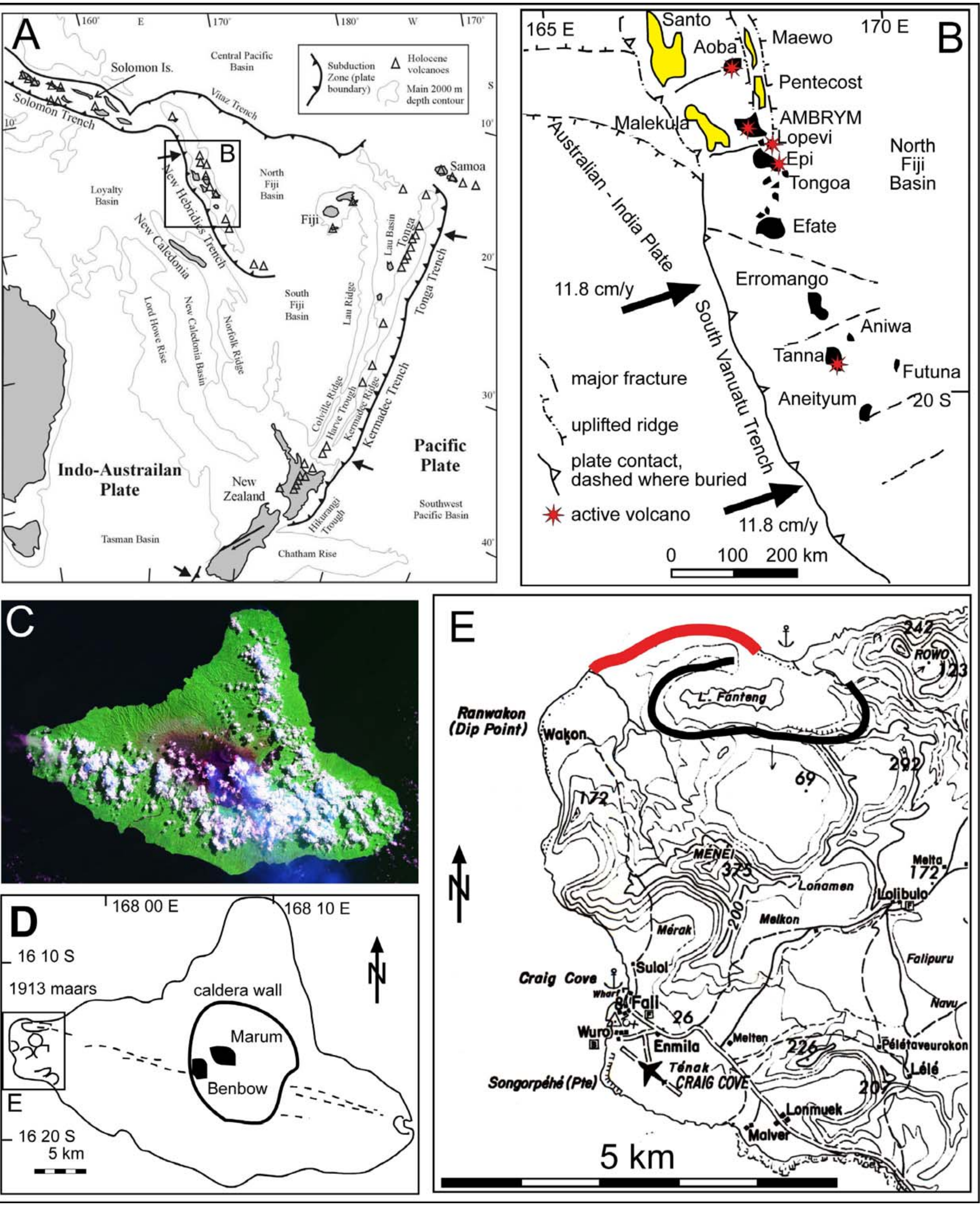
A
160°
E
170°
180°
W
170°
Solomon Is.
Central Pacific Basin
Subduction Zone (plate boundary)
Holocene volcanoes
Main 2000 m depth contour
Solomon Trench
Vitiaz Trench
S
10°
B
North Fiji Basin
Loyalty Basin
New Hebrides Trench
New Caledonia
Samoa
Fiji
Lau Basin
Tonga
Tonga Trench
20°
South Fiji Basin
Lau Ridge
Lord Howe Rise
New Caledonia Basin
Norfolk Ridge
30°
Colville Ridge
Harve Trough
Kermadec Ridge
Kermadec Trench
Pacific Plate
Indo-Austrailan Plate
New Zealand
Hikurangi Trough
Southwest Pacific Basin
Tasman Basin
Chatham Rise
40°
B
165 E
170 E
Santo
Aoba
Maewo
Pentecost
Malekula
AMBRYM
Lopevi
Epi
Tongoa
North Fiji Basin
Australian - India Plate
Efate
11.8 cm/y
Erromango
South Vanuatu Trench
Aniwa
Tanna
Futuna
Aneityum
20 S
major fracture
uplifted ridge
plate contact, dashed where buried
active volcano
11.8 cm/y
0
100
200 km
C
D
168 00 E
168 10 E
16 10 S
1913 maars
caldera wall
Marum
Benbow
E
16 20 S
5 km
N
E
242
ROWO
123
Ranwakon (Dip Point)
Wakon
L. Fanteng
292
69
172
MÉNÉI
375
Melta
172
Lonamen
Lolibulo
Melkon
200
Mérak
Falipuru
Craig Cove
Sulol
Wharf
Fall
26
Navu
Wuro
Enmila
Melten
226
Pélétaveurokon
Ténak
CRAIG COVE
Songorpéhé (Pte)
20
Lélé
Lonmuek
Malver
5 km
N

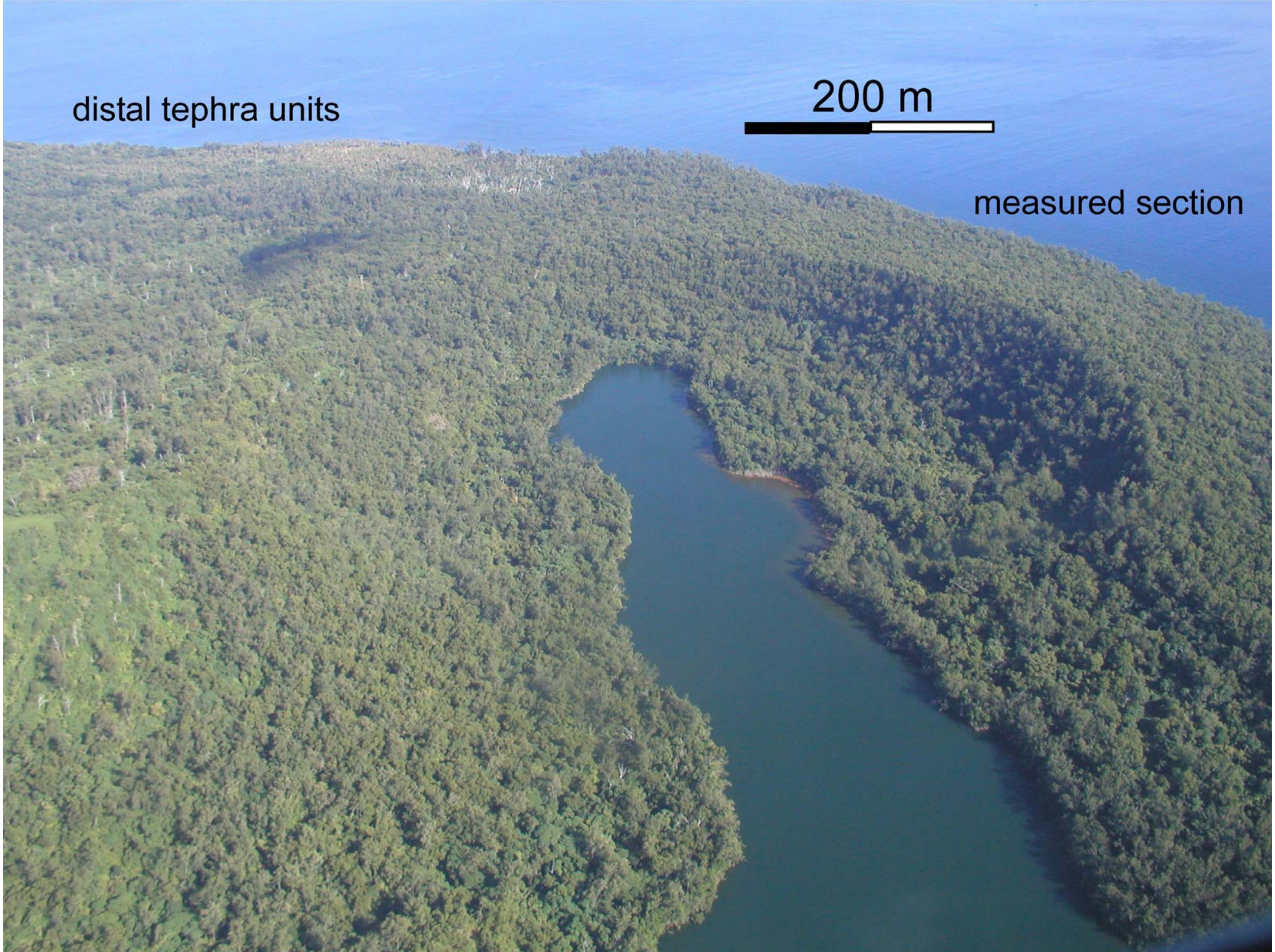
distal tephra units
200 m
measured section

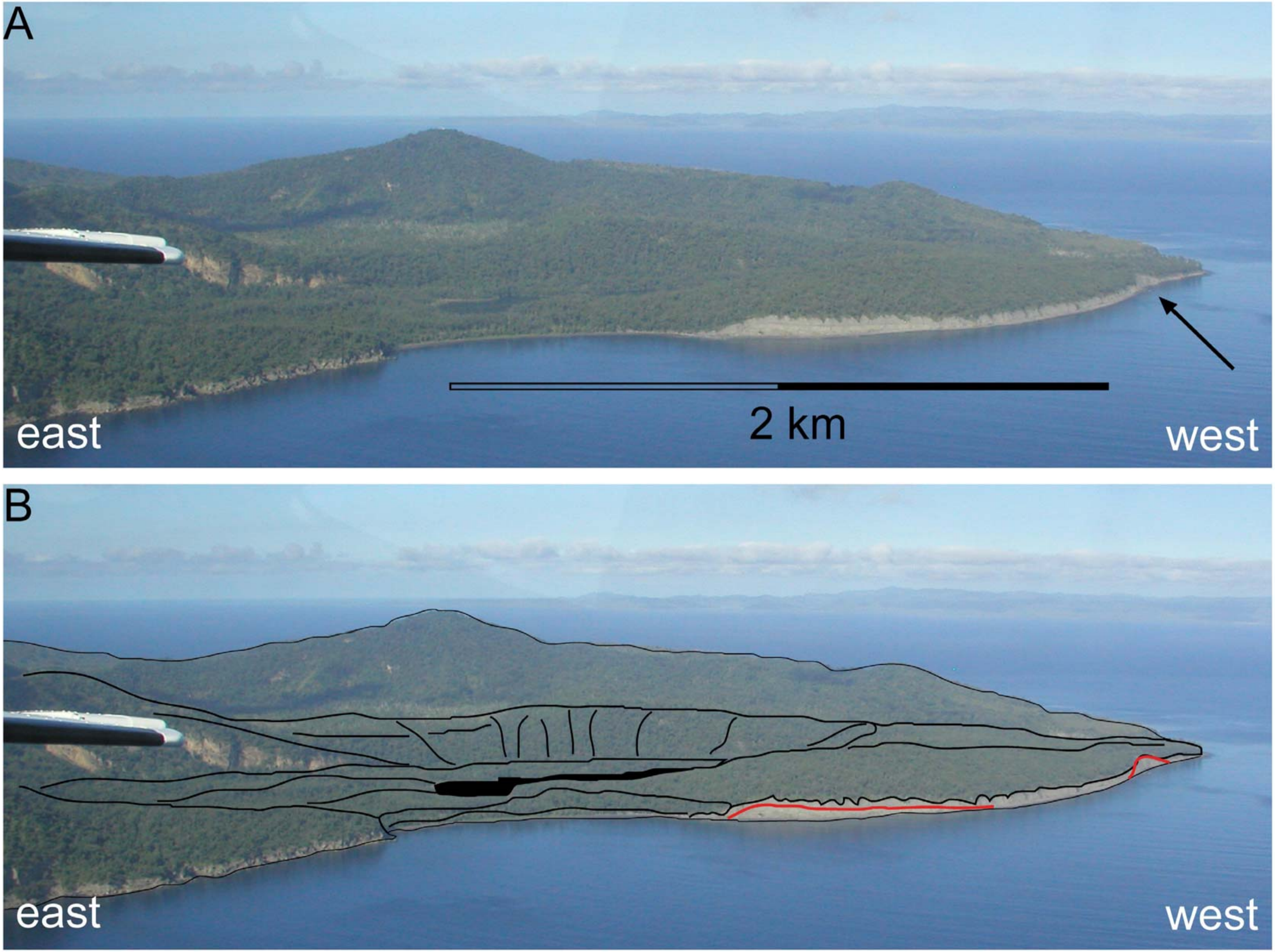
A
east
2 km
west
B
east
west

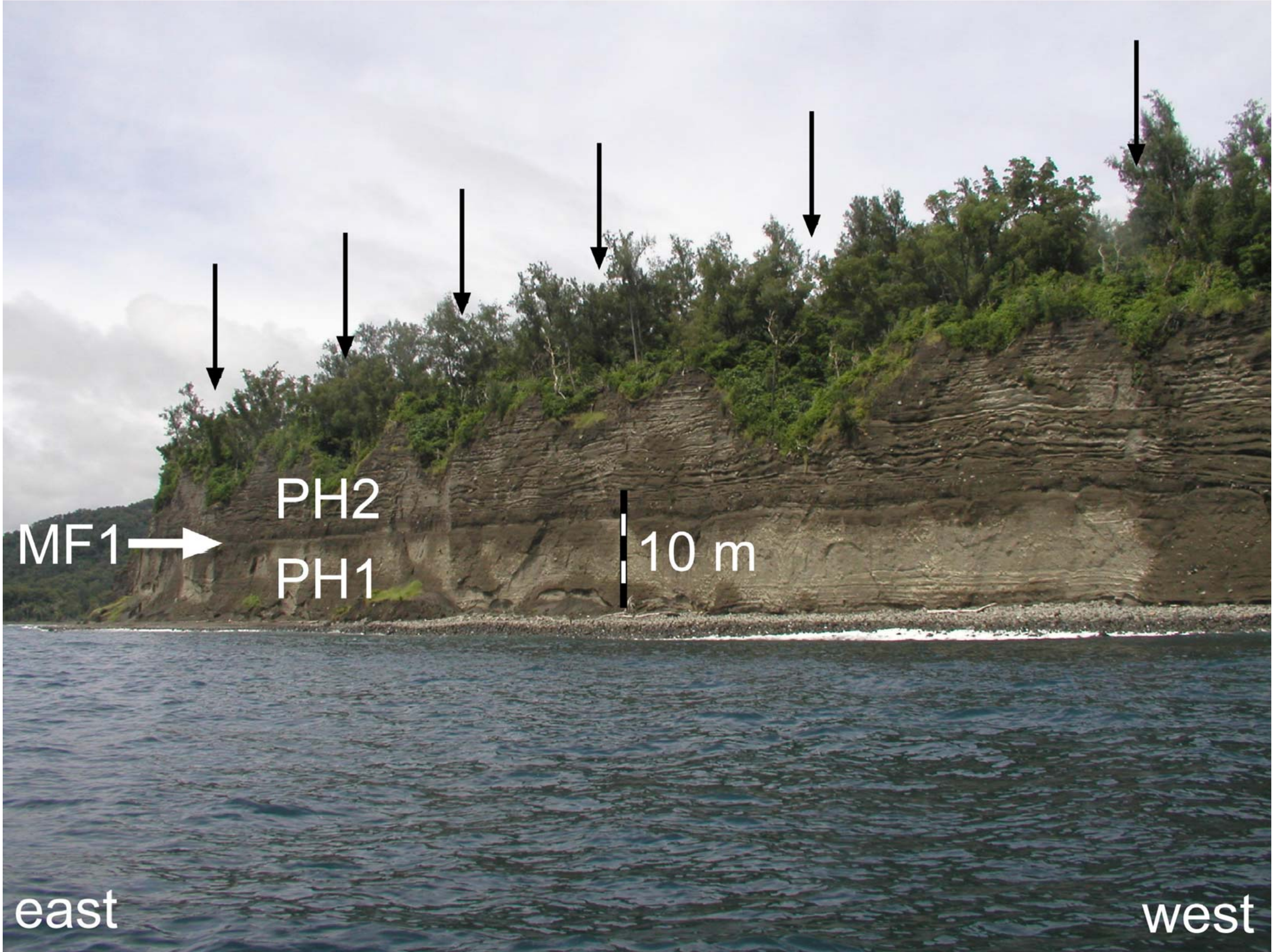
PH2
MF1
PH1
10 m
east
west

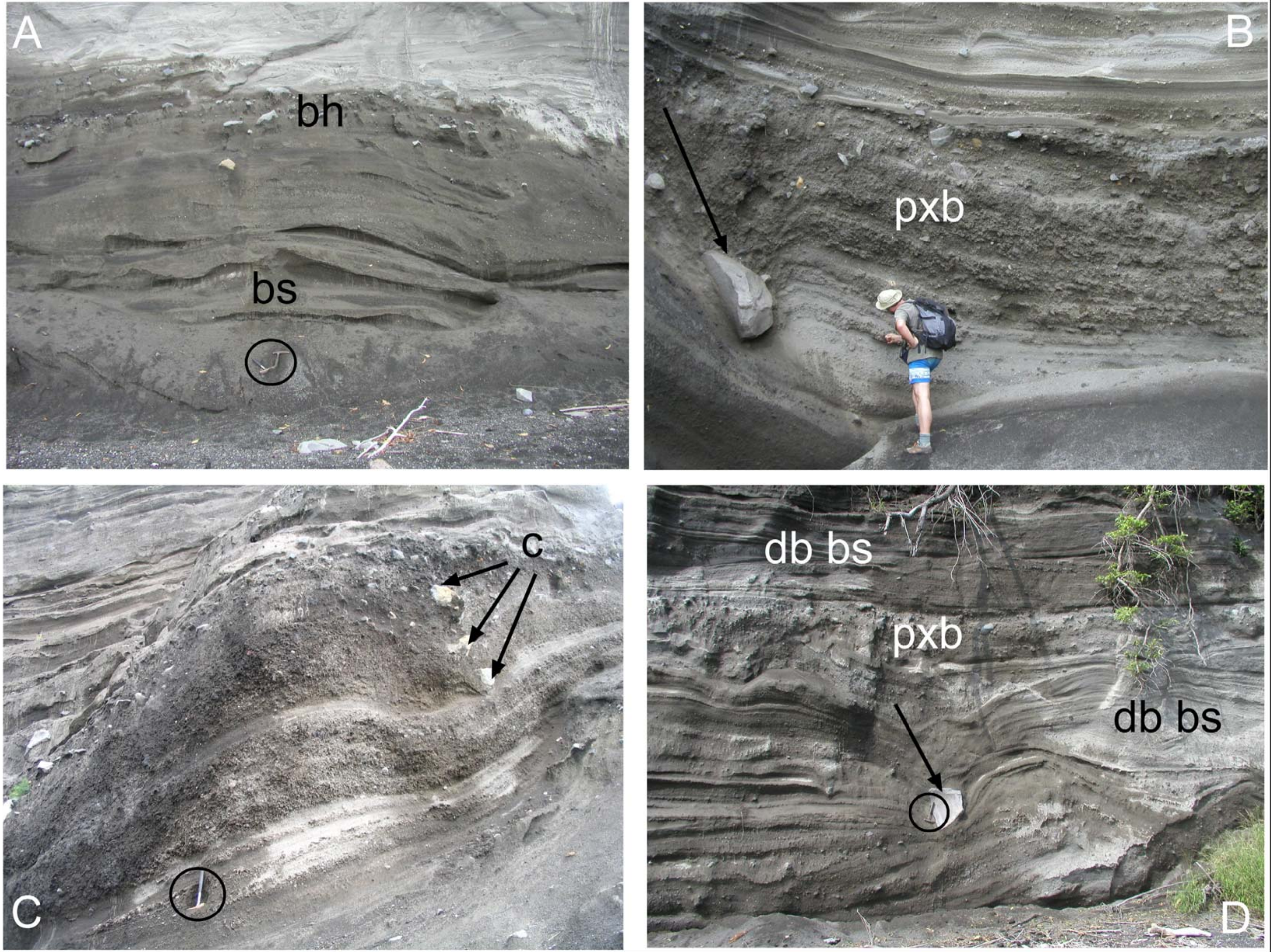
A
bh
bs
B
pxb
C
c
D
db bs
pxb
db bs

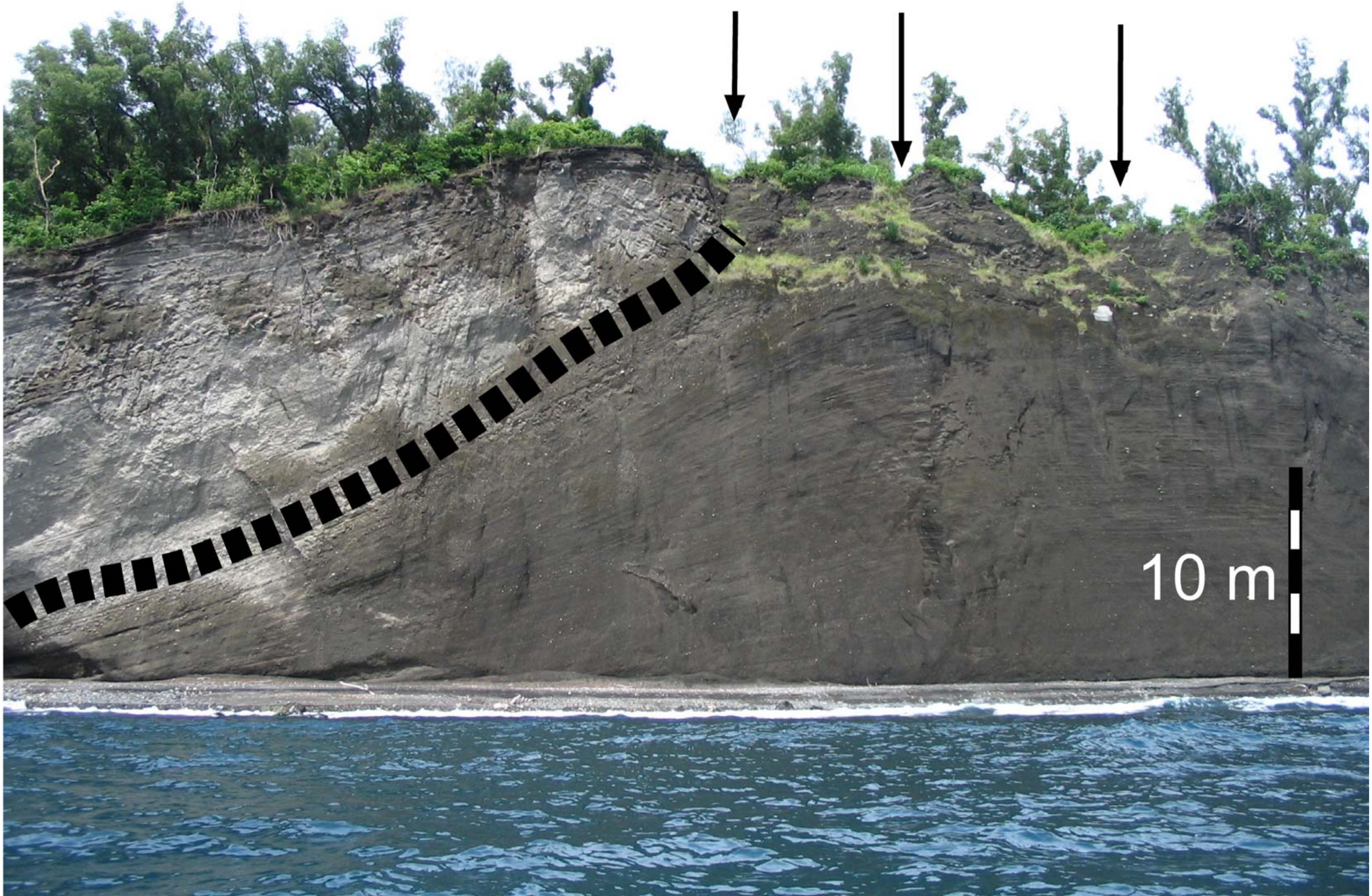
10 m


5 m
north-east
south-west

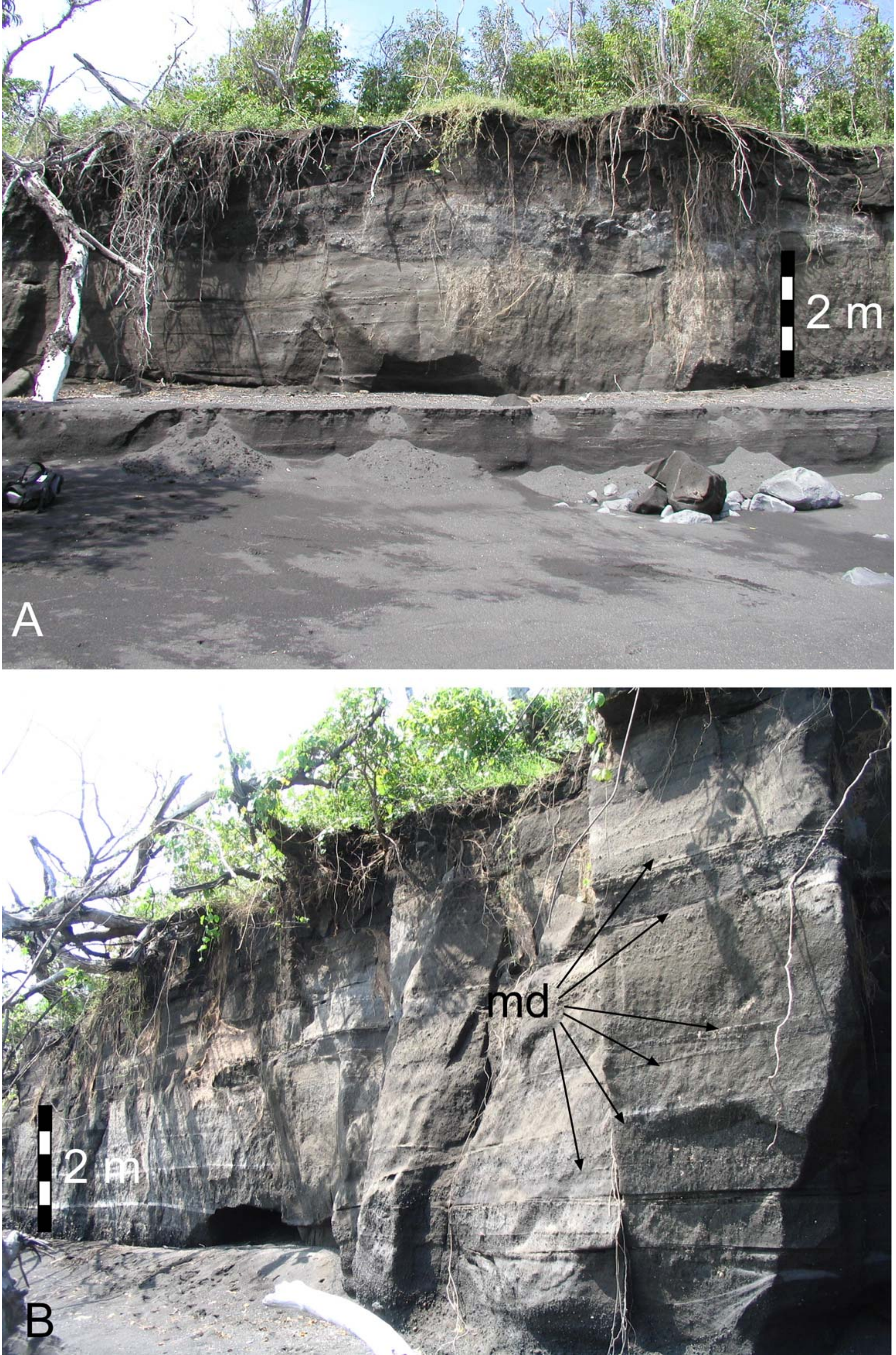
2 m
A
md
2 m
B

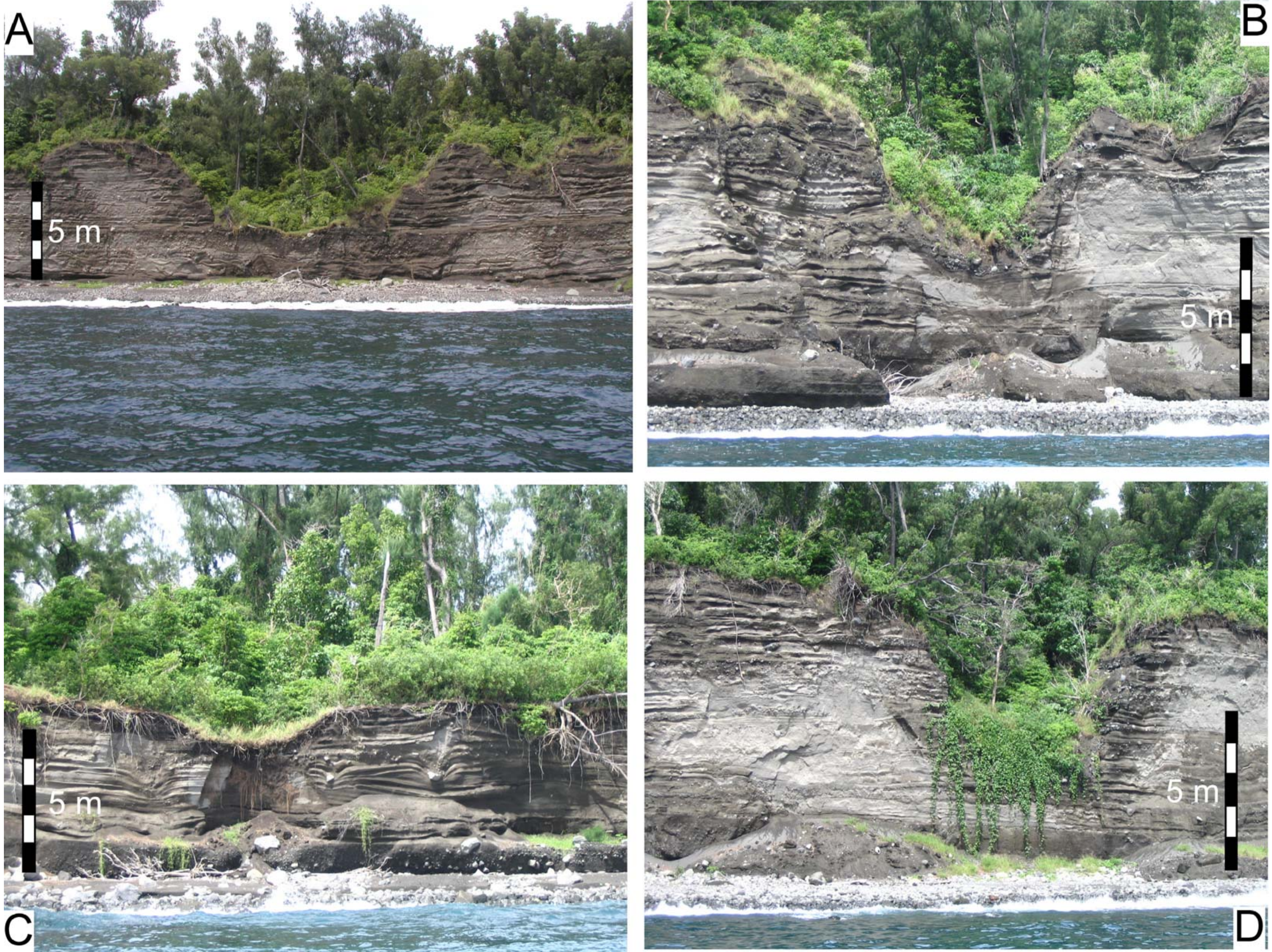
A
5 m
B
5 m
C
5 m
D
5 m

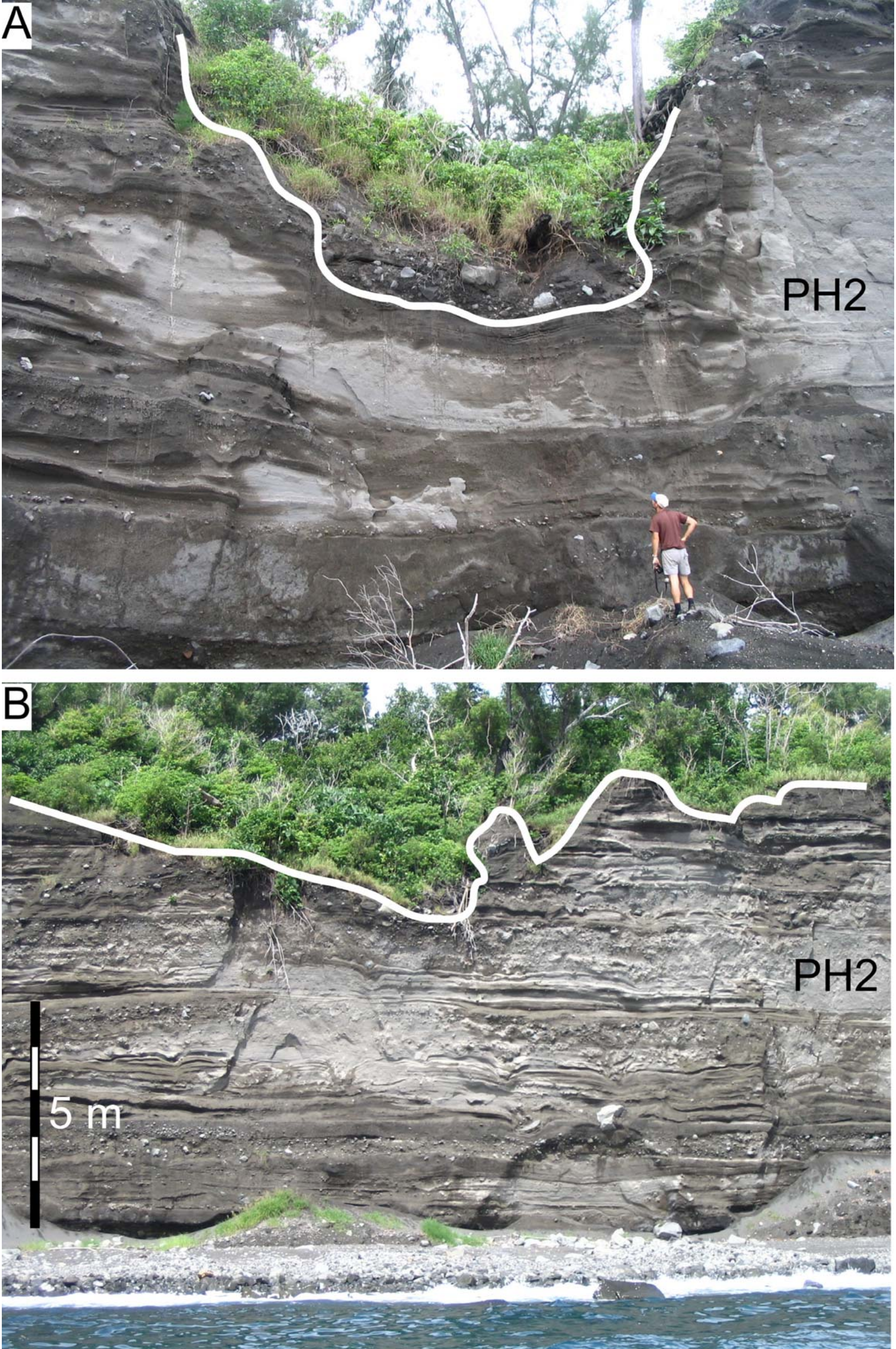
A
PH2
B
PH2
5 m


A
50 m
Wave cut shoreline
20 12 2005

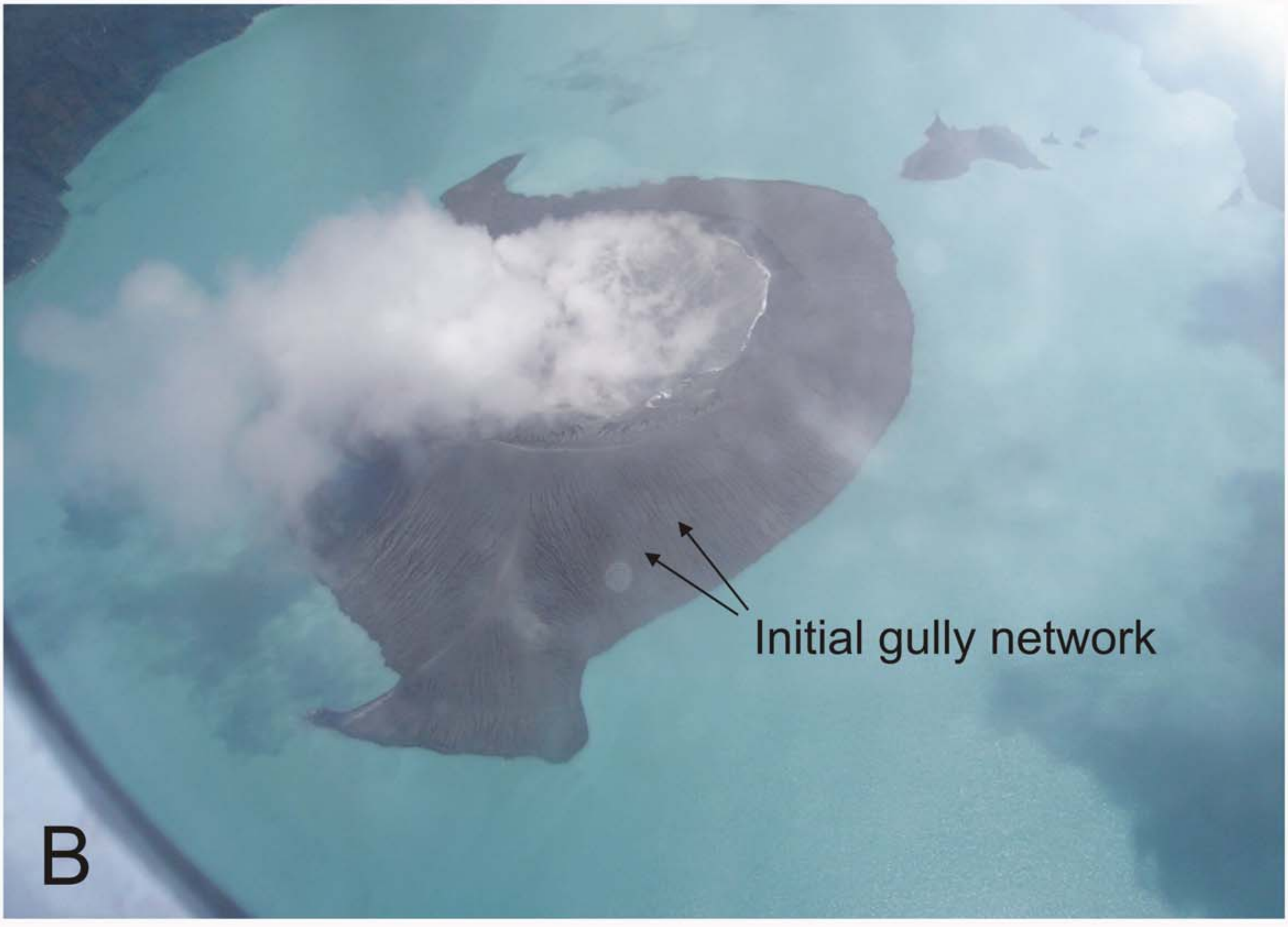
Initial gully network
B